

# Simulation of the Effect of Errors on the SNAP's Measurement of the Cosmological Parameters

Nick Mostek and Stuart Mufson  
Indiana University

July 31, 2001

## I. Introduction

We have constructed simple toy models to determine how experimental errors propagate into the precision that SNAP can achieve in its measurement of the cosmological parameters. Specifically, we investigate the impact of errors on the proposed SNAP mission objectives – measurement of  $\Delta\Omega_M/\Omega_M$  to  $\leq 2\%$  and the measurement of  $\Delta\Omega_\Lambda/\Omega_\Lambda$  to  $\leq 5\%$ . In this report, we consider three types of error: Gaussian distributed redshift errors, Gaussian distributed systematic errors, and non-Gaussian distributed systematic errors.

Gaussian distributed redshift errors are mostly the result of using photometry and low-resolution spectroscopy for the supernova redshift determination, rather than time-consuming, high-resolution spectroscopy. Gaussian distributed systematic errors and non-Gaussian distributed systematic errors are discussed in the document “Cosmological Parameters as a Function of  $z$ ” also found in this Yellow Book. As described there, Gaussian distributed systematic errors introduce ‘an irreducible systematic error that is independent of other redshift bins’. The K-correction is an example of this type of systematic. Non-Gaussian distributed systematic errors, on the other hand, are those which are ‘correlated systematic magnitude shifts’ that model errors introduced by supernova evolution, Malmquist bias, and gray dust.

## II. Toy Models

### A. Initial Cosmological Models

We analyzed the effect of errors on the cosmological models listed in Table 1.

Table 1. Input Cosmological Models

Model	$\Omega_M^0$	$\Omega_\Lambda^0$	$w^0$	
1	0.28	0.72	-0.7	flat
2	0.40	0.10	-0.7	mass dominated
3	0.28	0.30	-0.7	$\Omega_M \approx \Omega_\Lambda$
4	0.28	0.50	-0.7	$\Lambda$ dominated

In model 1 we assumed a flat universe prior so that the errors on the cosmological parameters are smaller. The curvature is unconstrained on the other models.

## B. Procedure

All our computations were based on Alex Kim's program SYSTEMATIC.PRO. However, the  $\chi^2$  minimization method was replaced by MINUIT, the well-known CERN minimization routine. In addition, the entire suite of routines was ported to the ROOT C++ framework to take advantage of the CERN histogramming, plotting, and analysis packages. We also used the routines in *Numerical Recipes* when required.

We investigated each error type individually. We then compared the results of superposing all the error types with our theoretical expectation.

### 1. Gaussian Redshift Errors

We first investigated how errors in redshift propagate into cosmological parameter errors in the absence of photometric measurement errors. The supernova distribution we used in this study was taken from Table 7.2 in the SNAP proposal. In particular, we chose 2,366 supernova redshifts  $z_i$ , by a Monte Carlo method that preserves the number of supernova in each redshift bin of the table (width  $\Delta z = 0.1$ ) and which assumes a linear increase in the number of supernova in each bin. Current instrumental designs for SNAP are now being considered that will follow even more supernovae.

For each input cosmology, we first computed the distance moduli,

$(m - M)_i = \mathbf{m}_i(z_i, \Omega_M^0, \Omega_\Lambda^0, w^0)$ , for the supernovae, where "0" indicates the initial model parameters. We then chose a normally distributed redshift error,  $\delta z_i$ , for each supernova using a constant standard deviation  $\sigma_z$  in the range  $\mathbf{s}_z = 0.001-0.01$ , and used MINUIT to minimize the statistic

$$\mathbf{c}^2 = \sum_{i=1}^{2,366} [\Delta M_B^0 + \mathbf{m}_i(z_i + \mathbf{d}z_i, \Omega_M, \Omega_\Lambda, w) - \mathbf{m}_i(z_i, \Omega_M^0, \Omega_\Lambda^0, w^0) - \mathbf{a}s^0 \times \mathbf{d}z_i / (1 + z_i)]^2 / \mathbf{s}_i^2$$

for the best-fitting cosmological parameters  $\Omega_M, \Omega_\Lambda, w$ , and  $\Delta M_B^0$ . In this expression,  $\Delta M_B^0 = M_B - M_B^0$  measures the best-fit SNIa absolute magnitude compared with the input absolute magnitude. For each supernova, the phenomenological stretch correction is given by the relation  $\mathbf{D}m = \mathbf{a}(s-1)$ . Since  $\mathbf{D}m$  must be corrected for time dilation, the error in the stretch correction is written  $\Delta s = \mathbf{a}s^0 \times \mathbf{d}z / (1 + z)$ . In this computation, we used  $\alpha = -1.74$  and  $s^0 = 1$ . The factor  $\mathbf{s}_i$  represents the photometric error and is constant since all supernovae will have the same quality observations. In our computations, MINUIT minimizes  $\chi^2$  with respect to four fit parameters,  $\mathbf{W}_M, \mathbf{W}_L, w$ , and  $\Delta M_B^0$ , and we allowed these parameters to vary over the ranges shown in Table 2.

Table 2. Allowed Ranges for Fit Parameters in MINUIT

$0.1 \leq \Omega_M \leq 0.55$	$-1.0 \leq \Omega_\Lambda \leq 1.0$	$-1.0 \leq w \leq 0$	$-0.1 \leq dM_B^0 \leq 0.1$
-------------------------------	-------------------------------------	----------------------	-----------------------------

We repeated this process for 200 trials for each input cosmology and made histograms of the quantities  $\Delta\Omega_M = \langle\Omega_M\rangle - \Omega_M^0$ ,  $\Delta\Omega_\Lambda = \langle\Omega_\Lambda\rangle - \Omega_\Lambda^0$ ,  $\Delta w = \langle w\rangle - w^0$ , and  $\Delta M_B^0$ . We then increased the input standard deviation,  $\mathbf{s}_z$ , and repeated the computations. Examples of these histograms for the four input cosmologies and  $\mathbf{s}_z = 0.003$  are shown in Figures 1a, 1b, 1c, and 1d.

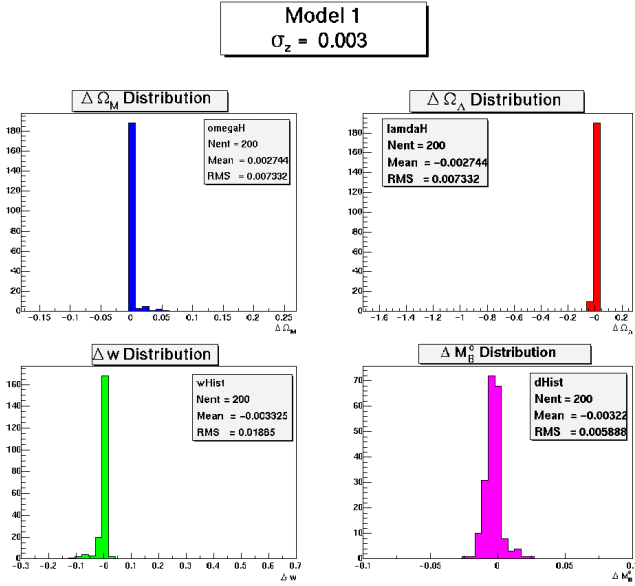


Figure 1a

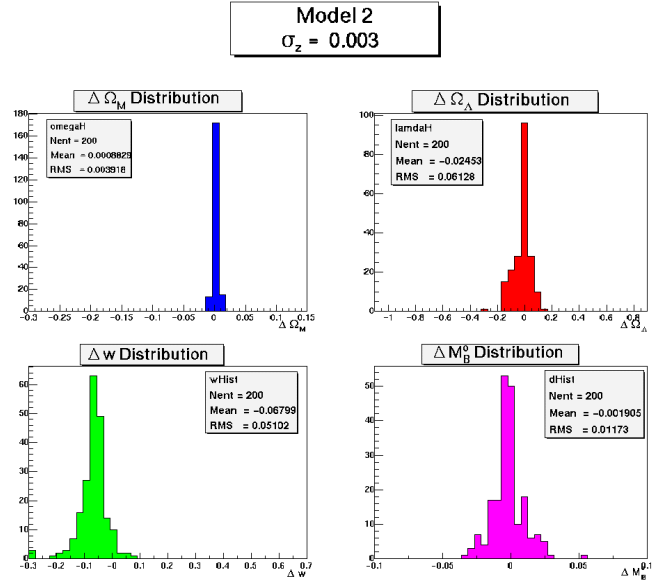


Figure 1b

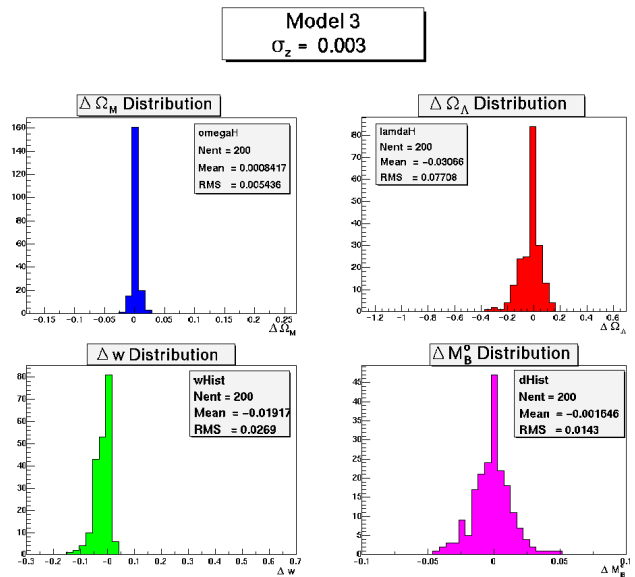


Figure 1c

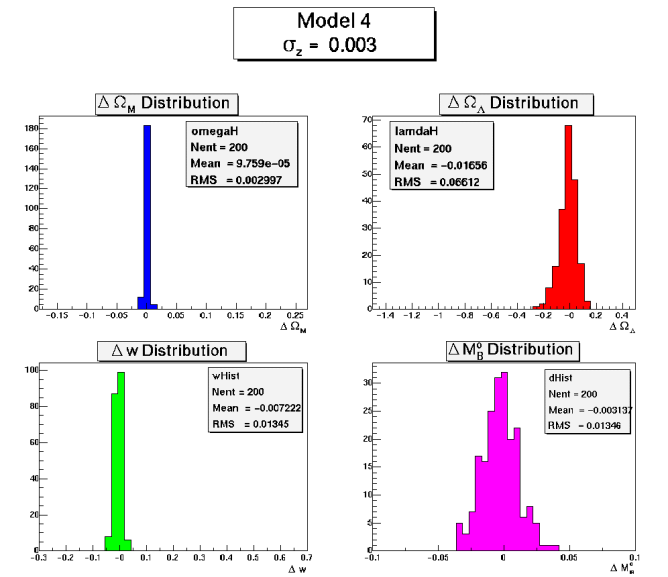


Figure 1d

## 2. Gaussian Systematic Errors

For these computations we used one supernova in each of 170 redshift bins of width  $\Delta z = 0.01$ , and we assumed that the redshifts of these supernovae were at the bin midpoint. For each initial cosmological model, we first chose the standard deviation for the photometric errors in each redshift bin,  $\mathbf{s}_m(z)$ , according to the relation

$$\mathbf{s}_m(z) = \Delta m_{\max} \times z / 1.7,$$

where  $\Delta m_{\max}$  is in the range 0.005-0.035 magnitudes, and then determined a normally distributed error in the measured magnitude,  $\mathbf{D}m_i$ , for each supernova in the study. We used MINUIT to find the best-fitting cosmological parameters  $\Omega_M, \Omega_\Lambda, w$ , and  $\Delta M_B^0$  by minimizing the statistic

$$\chi^2 = \sum_{i=1}^{170} \left\{ \Delta M_B^0 + \mathbf{m}_i(z_i, \Omega_M, \Omega_\Lambda, w) - [\mathbf{m}_i(z_i, \Omega_M^0, \Omega_\Lambda^0, w^0) + \Delta m_i(z_i)] \right\}^2 / \mathbf{s}_i^2.$$

We varied the parameters over the same ranges as in the case of statistical errors. We repeated this process for 500 trials for each choice of cosmological model and mean magnitude error, and computed the relevant histograms. We repeated this process for 500 trials for each input cosmology and made histograms of the quantities  $\Delta \Omega_M = \langle \Omega_M \rangle - \Omega_M^0$ ,  $\Delta \Omega_\Lambda = \langle \Omega_\Lambda \rangle - \Omega_\Lambda^0$ ,  $\Delta w = \langle w \rangle - w^0$ , and  $\Delta M_B^0$ . We then increased the standard deviation,  $\mathbf{s}_m(z_{\max})$ , and repeated the computations.

## 3. Non-Gaussian Systematic Errors

For these computations we used one supernova in each of 170 redshift bins of width  $\Delta z = 0.01$ . We assumed that the redshifts of the supernovae were at the bin midpoint.

For each initial cosmological model, we chose a systematic photometric offset in each redshift bin according to the relation

$$\langle \Delta m(z) \rangle = \Delta m_{\max} \times z / 1.7,$$

where  $\Delta m_{\max}$  is in the range 0.005-0.035 magnitudes. In this case, the offset was applied directly to the measured magnitude for a single supernova at the center of each redshift bin. We used MINUIT to find the best-fitting cosmological parameters  $\Omega_M, \Omega_\Lambda, w$ , and  $\Delta M_B^0$ . We varied the fit parameters over the same ranges as in the previous cases and minimized the same  $\chi^2$  as in the case of Gaussian systematic errors. Since the errors are always the same, there is no need to repeat the process.

### III. Results

#### A. Gaussian Redshift Errors

Figures 2a, 2b, 2c, and 2d show the rms of the distributions for 200 trials as a function of the mean redshift error for the four input cosmologies. In Figures 3a, 3b, 3c, and 3d, we show the deviation from the mean as a function of the mean redshift error for the four models. The error bars in Figures 3 represent the errors in the mean. On Figures 2a-d, straight line fits to the rms as a function of mean redshift errors is superposed for range in which the fits are appropriate. On these figures the fit parameters are also shown. In the construction of these figures, significant outliers were excluded.

For the flat case 1, shown in Figures 2a and 3a, the rms increases linearly until  $s_z \approx 0.008$ , and then flattens out. In this case, deviations from the mean are  $<1\%$  and insignificant. For the matter dominated case 2, shown in Figures 2b and 3b, the rms increases linearly for  $\Delta\Omega_M$  and  $\Delta w$  for all values of  $s_z$ . On the other hand, for  $DW_L$  and  $\Delta M_B^0$ , the rms increases linearly until  $s_z \approx 0.008$ , and then begins to deviate quite considerably from the linear increase for larger errors. As can be seen from Figure 3b,  $DW_L$  and  $Dw$  deviate considerably from their initial values for larger errors. What appears to be happening in the mass dominated cosmologies with large redshift errors, the solutions for  $\Omega_\Lambda$  that MINUIT finds are not well constrained. Basically MINUIT finds solutions that tend toward  $W_L \gg 0$  when the redshift errors are large. In addition, since  $\Omega_\Lambda$  is small,  $w$  will not be well determined and MINUIT continually runs up against its  $w = -1$ . As shown in Figures 2c and 3c, this behavior is still in evidence for the  $W_M \gg W_L$  but it is not quite so strong. For the  $W_L$  dominant case, shown in Figures 2d and 3d, the behavior is somewhat different. In this case, MINUIT finds solutions tending toward larger values of  $W_L$  as redshift errors become large. However, since  $W_L$  is dominant,  $Dw$  is not as large as in the previous cases.

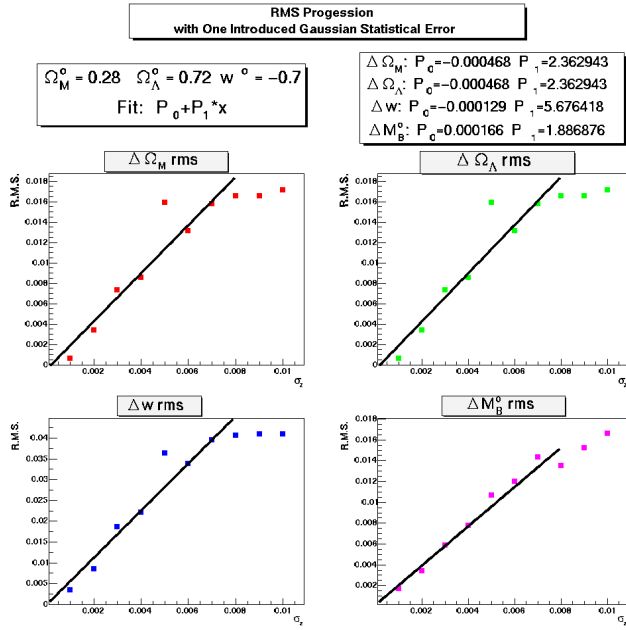


Figure 2a

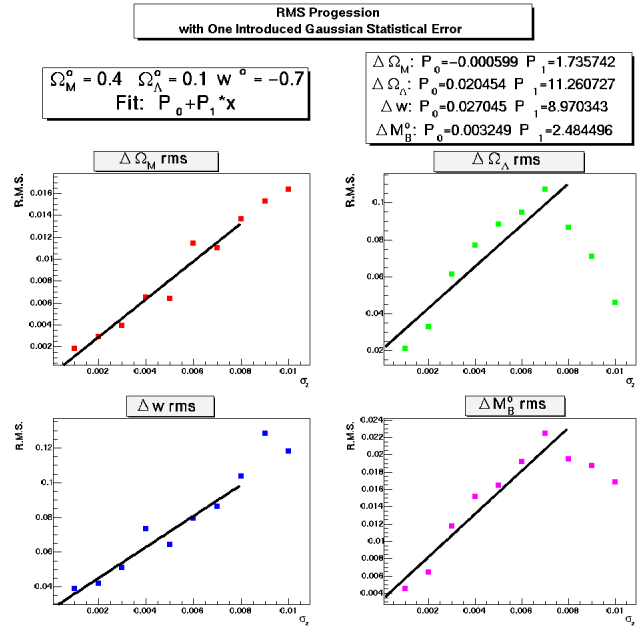


Figure 2b

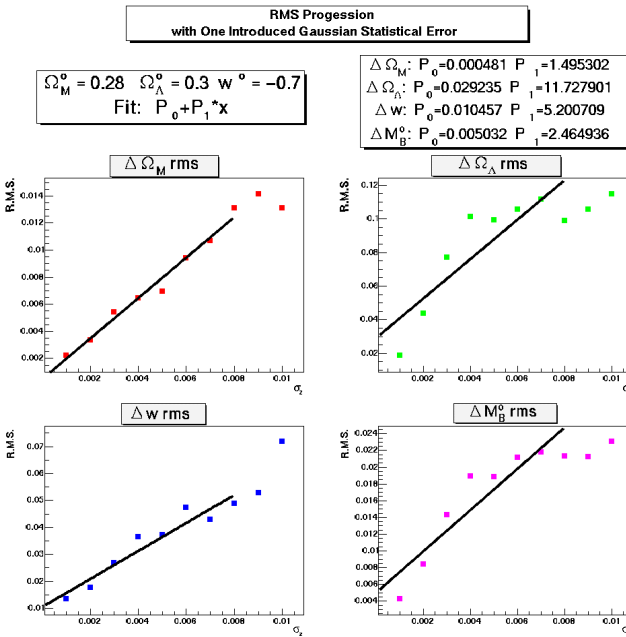


Figure 2c

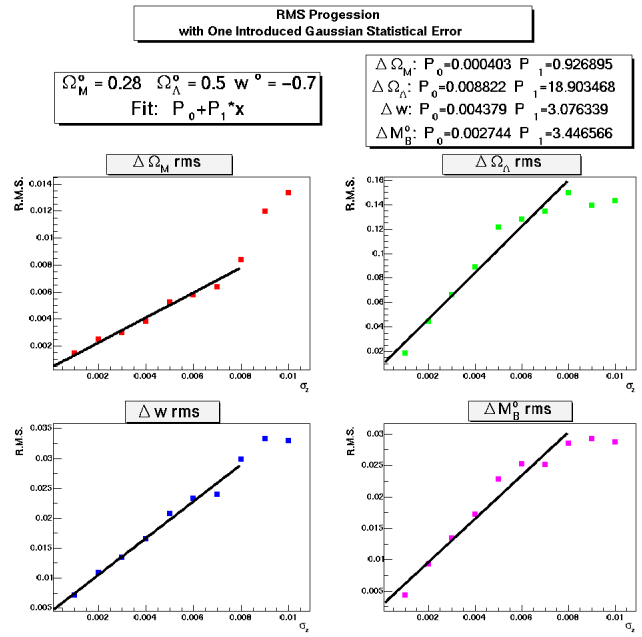


Figure 2d

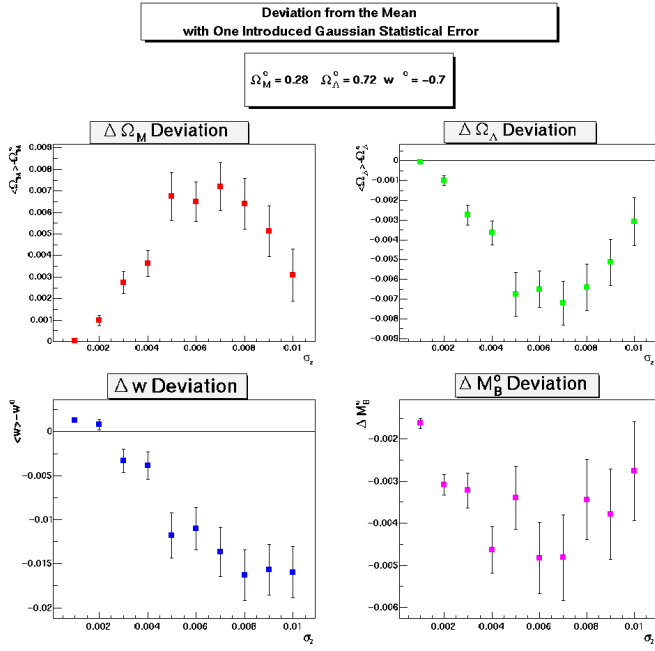


Figure 3a

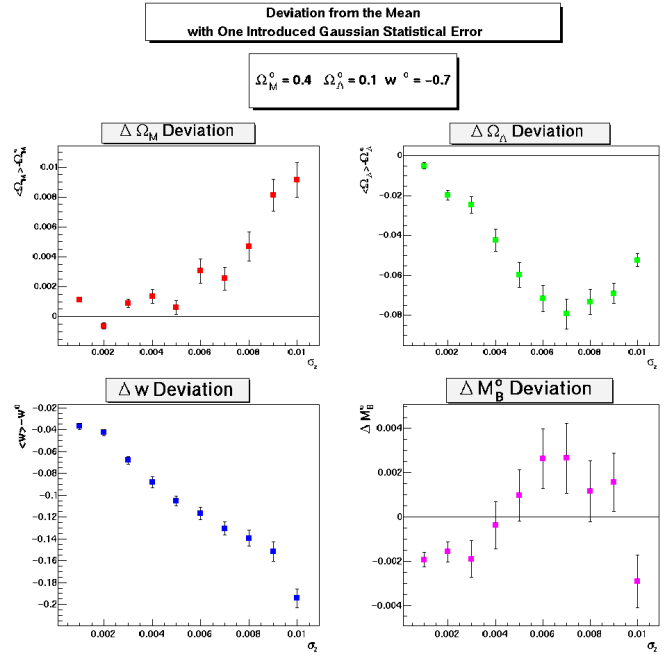


Figure 3b

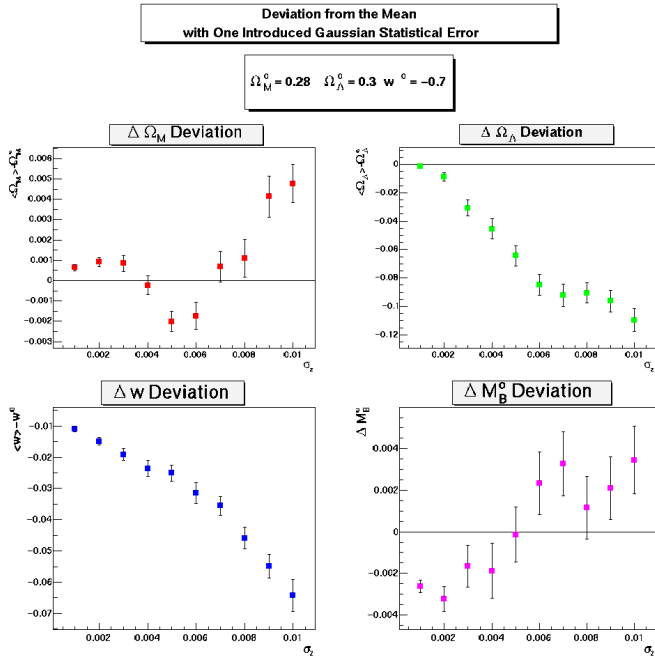


Figure 3c

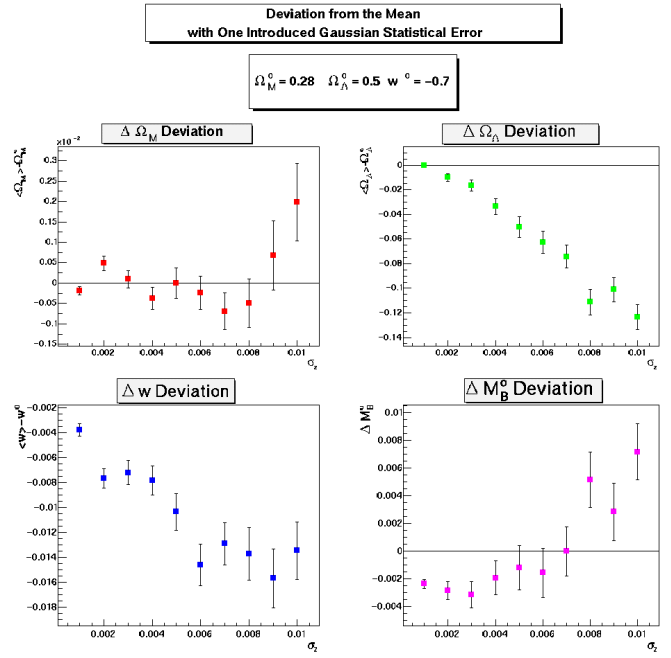


Figure 3d

## B. Gaussian Systematic Errors

Figures 4a, 4b, 4c, and 4d show the r.m.s. of the distributions for 500 trials as a function of the magnitude of  $\Delta m_{max}$  for the four input cosmologies. The rms of the parameter distributions clearly increase linearly over the range of  $\Delta m_{max}$  studied. Except in one instance, the deviations from the mean of the cosmological parameters are  $< 0.01$  for this error type; that is, within computational errors,  $\langle \Omega_M \rangle - \Omega_M^0 \approx 0$ ,  $\langle \Omega_\Lambda \rangle - \Omega_\Lambda^0 \approx 0$ ,  $\langle w \rangle - w^0 \approx 0$ , and  $\langle \Delta M_B^0 \rangle \approx 0$ . For model 2,  $\langle w \rangle - w^0 \approx 0.05$  for  $\Delta m_{max} = 0.035$ .

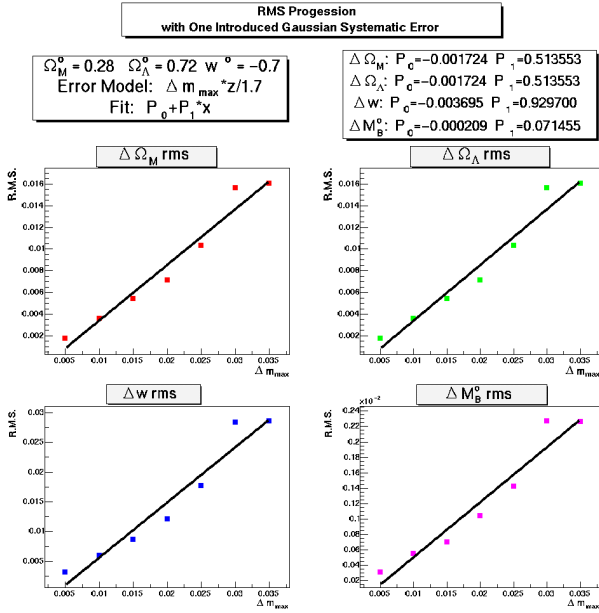


Figure 4a

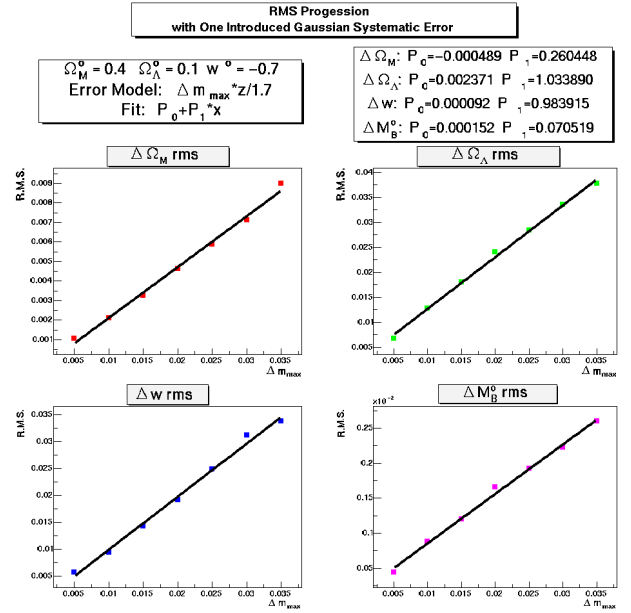


Figure 4b

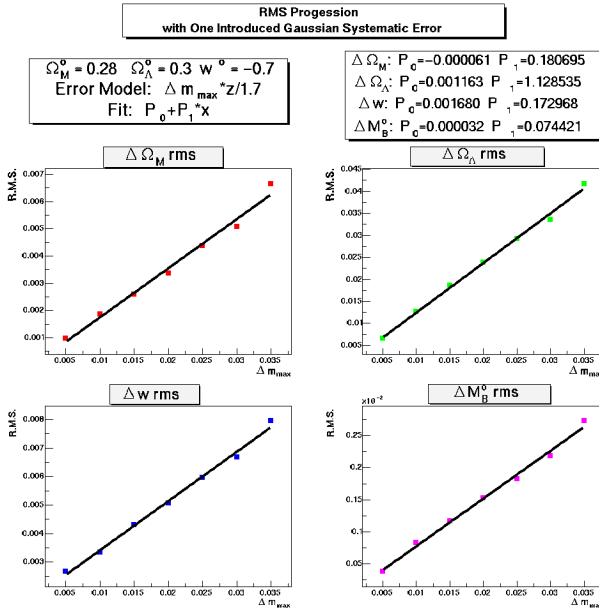


Figure 4c

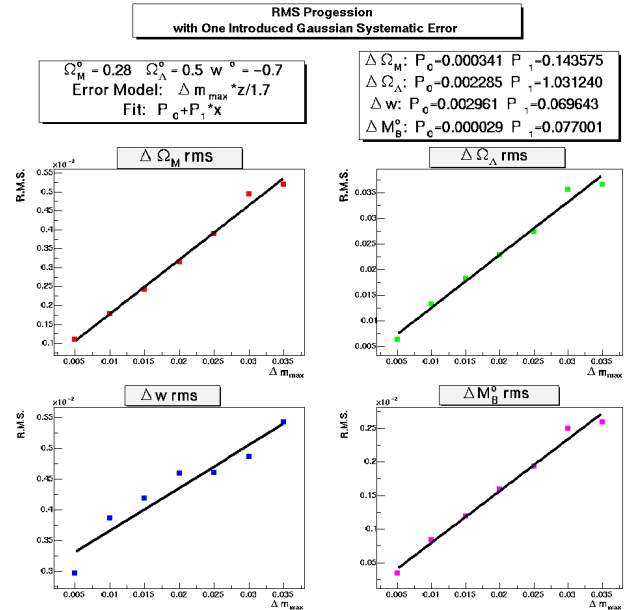


Figure 4d



### C. Non-Gaussian Systematic Errors

Figures 5a, 5b, 5c, and 5d show the deviation from the mean of the cosmological parameters as a function of the magnitude of  $\Delta m_{\max}$  for the four input cosmologies. The deviations in  $\Delta M_B^0$  are small and insignificant for all input cosmologies. For the flat case model 1, the deviations  $\langle \Omega_M \rangle - \Omega_M^0$  increase with  $Dm_{\max}$ ; in addition, the behavior is highly variable for the largest values of  $Dm_{\max}$ . For the remaining input cosmologies,  $\langle \Omega_M \rangle - \Omega_M^0$  decreases with increasing  $Dm_{\max}$ . Similar behavior is also seen for  $\langle w \rangle - w^0$ , except that  $\langle w \rangle - w^0 \approx 0$  for small values of  $Dm_{\max}$ . The deviations  $\langle \Omega_\Lambda \rangle - \Omega_\Lambda^0$  decrease for all input cosmologies. In model 4 it appears as if MINUIT is making a transition to a different minimum in parameter space as  $Dm_{\max}$  increases.

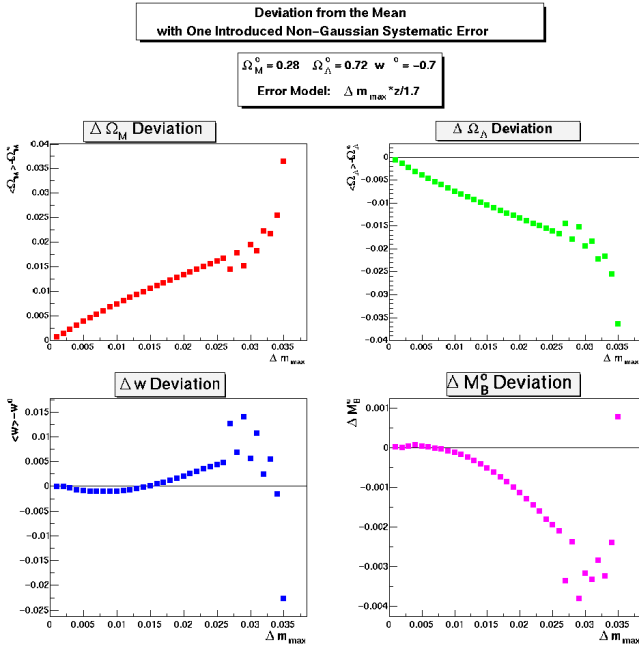


Figure 5a

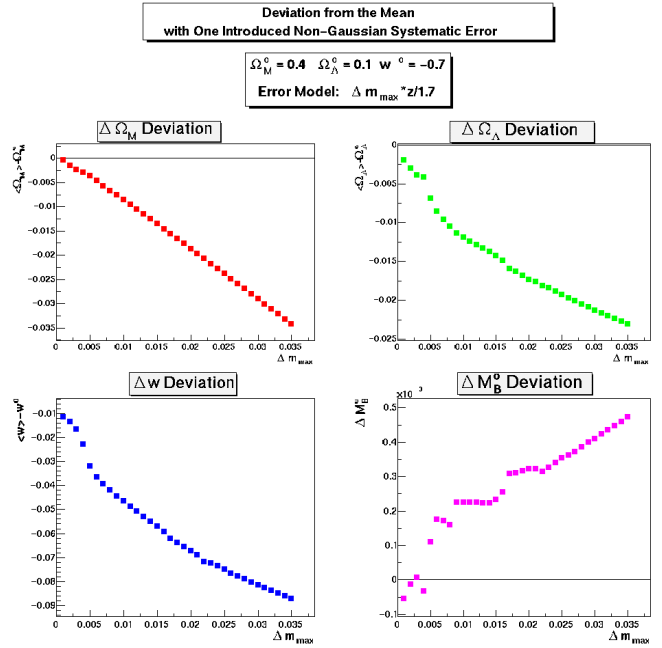


Figure 5b

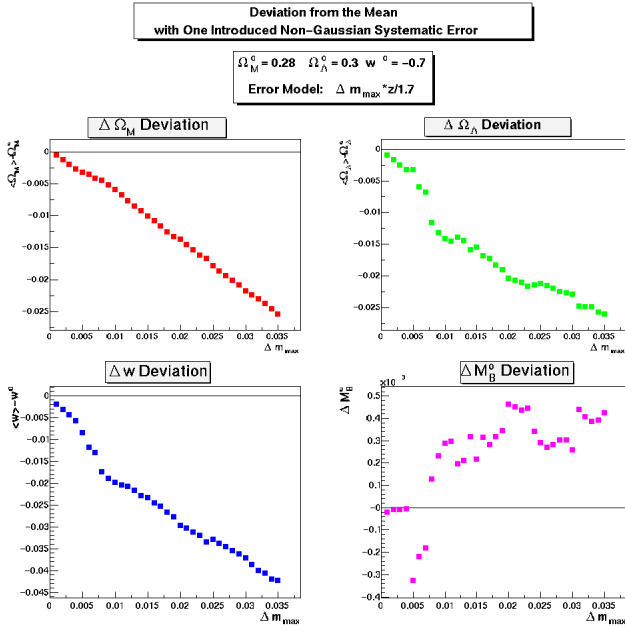


Figure 5c

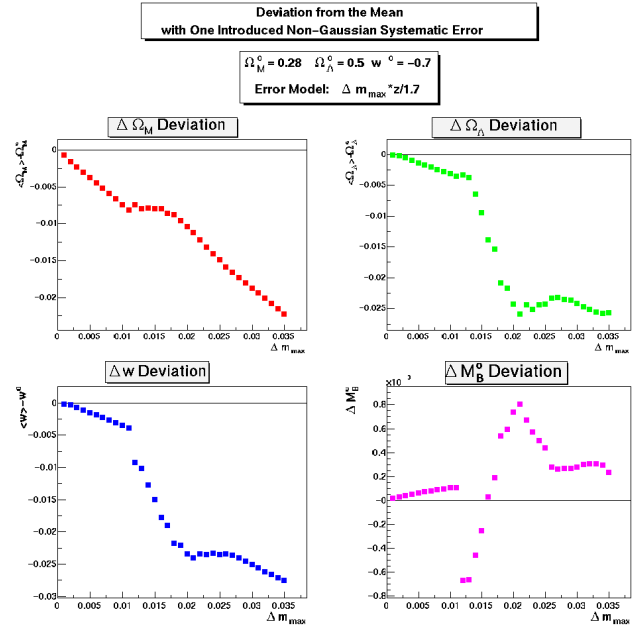


Figure 5d

## D. Models with Multiple Error Types

Using the results above we can compute the combined effect of multiple error types on the cosmological parameters. We first determine the rms for the combined model by adding the rms of the Gaussian statistical errors and the Gaussian systematic errors in quadrature. We then compute the deviation from the mean for the cosmological parameters by simply adding the deviation from the mean for the non-Gaussian systematic errors.

We tested this hypothesis by running 200 trials each for a combined error case. For these computations we chose redshift errors as in the Gaussian statistical error case for the 2,366 SNIa. We chose a Gaussian systematic error using

$$s_m(z) = \Delta m_{\max} \times z/1.7,$$

and a non-Gaussian systematic error in the supernova magnitude using

$$\langle \Delta m(z) \rangle = \Delta m_{\max} \times z/1.7.$$

We then used MINUIT to find the best-fitting cosmological parameters by minimizing the statistic

$$c^2 = \sum_{i=1}^{2,366} [\Delta M_B^0 + \mathbf{m}_i(z_i + \mathbf{d}z_i, \Omega_M, \Omega_\Lambda, w) - \mathbf{m}_i(z_i, \Omega_M^0, \Omega_\Lambda^0, w^0) - \Delta m_i(z_i) - \mathbf{a} s^0 \times \mathbf{d}z_i / (1 + z_i)]^2 / \mathbf{s}_i^2$$

We show the results of the computations in Figures 6. We summarize the results in Table 3 below. For this case the predictions match the computations quite well.

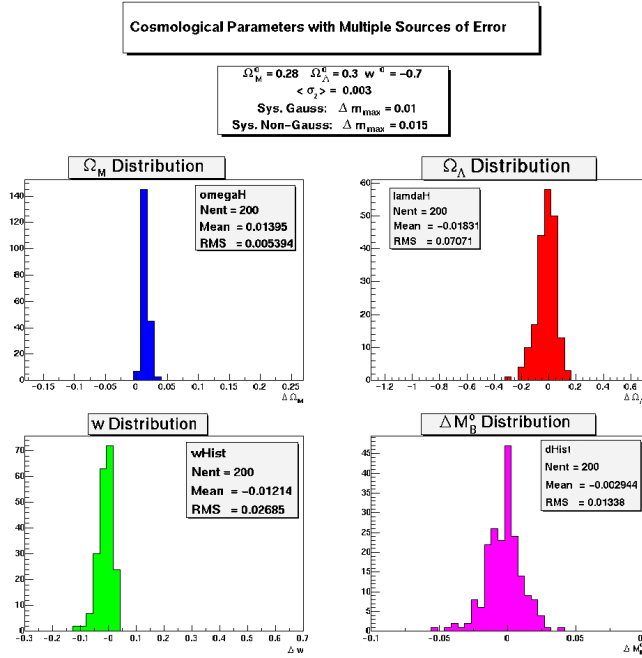


Figure 6

Table 3. Combined Error Model

Model	3
Gaussian Statistical	.003
Gaussian Systematic	.01
Non-Gaussian Statistical	.015
$\mathbf{s}(\Omega_M)_{pred} - \mathbf{s}(\Omega_M)_{comp}$	$\approx 0$
$[\langle \Omega_M \rangle - \Omega_M^0]_{pred} - [\langle \Omega_M \rangle - \Omega_M^0]_{comp}$	.001
$\mathbf{s}(\Omega_\Lambda)_{pred} - \mathbf{s}(\Omega_\Lambda)_{comp}$	.006
$[\langle \Omega_\Lambda \rangle - \Omega_\Lambda^0]_{pred} - [\langle \Omega_\Lambda \rangle - \Omega_\Lambda^0]_{comp}$	.001
$\mathbf{s}(w)_{pred} - \mathbf{s}(w)_{comp}$	.002
$[\langle w \rangle - w^0]_{pred} - [\langle w \rangle - w^0]_{comp}$	.01
$\mathbf{s}(dM_B^0)_{pred} - \mathbf{s}(dM_B^0)_{comp}$	$\approx 0$
$\langle dM_B^0 \rangle_{pred} - \langle dM_B^0 \rangle_{comp}$	$\approx 0$